Energy filtering transmission electron microscopy immunocytochemistry and antigen retrieval of surface layer proteins from Tannerella forsythensis by microwave or autoclave heating with citraconic anhydride

Journal:	*Biotechnic & Histochemistry*
Manuscript ID:	TBIH-2011-0028.R3
Manuscript Type:	Technical Notes
Date Submitted by the Author:	09-Dec-2011
Complete List of Authors:	Moriguchi, Keiichi; Aichi-Gakuin University, Oral Anatomy
Keywords:	antigen retrieval technique, immunolabelling study, Tannerella forsythensis

For Peer Review Only

SCHOLARONE™
Manuscripts

Running head: Antigen retrieval and EFTEM immunocytochemistry

Address for correspondence:

Keiichi Moriguchi

Department of Oral Anatomy

School of Dentistry

Aichi Gakuin University

Nagoya 464-8650, Japan.

e-mail: keiichi@dpc.aichi-gakuin.ac.jp

For Peer Review Only

Energy filtering transmission electron microscopy immunocytochemistry and antigen retrieval of surface layer proteins from *Tannerella forsythensis* using microwave or autoclave heating with citraconic anhydride

K Moriguchi[1,5], Y Mitamura[2], J. Iwami[3], Y Hasegawa[4], N Higuchi[3,5], Y Murakami[4], H Maeda[2,5], F Yoshimura[4], H Nakamura[3,5], N Ohno[1,5]

Departments of [1]Oral Anatomy,[2]Oral Pathology, [3]Endodontics, [4]Microbiology, School of Dentistry, Aichi Gakuin University, Nagoya, Aichi 464-8650, [4]Oral Microbiology, Division of Oral Infections and Health Sciences, Asahi University School of Dentistry, 1851 Hozumi, Mizuho, Gifu 501-0296, and [5]Research Institute of Advanced Oral Science, School of Dentistry, Aichi Gakuin University, Nagoya, Aichi 464-8650 Japan

Accepted October 18, 2011

For Peer Review Only

Abstract

Tannerella forsythensis (*Bacteroides forsythus*), an anaerobic Gram-negative species of bacteria that plays a role in the progression of periodontal disease, has a unique bacterial protein profile. It is characterized by two unique protein bands with molecular weights of more than 200 kDa. It also is known to have a typical surface layer (S-layer) consisting of regularly arrayed subunits outside the outer membrane. We examined the relationship between high molecular weight proteins and the S-layer using electron microscopic immunolabeling with chemical fixation and an antigen retrieval procedure consisting of heating in a microwave oven or autoclave with citraconic anhydride. Immunogold particles were localized clearly at the outermost cell surface. We also used energy-filtering transmission electron microscopy (EFTEM) to visualize 3, 3'-diaminobenzidine tetrahydrochloride (DAB) reaction products after microwave antigen retrieval with 1% citraconic anhydride. The three-window method for electron spectroscopic images (ESI) of nitrogen by the EFTEM reflected the presence of moieties demonstrated by the DAB reaction with horseradish peroxidase (HRP)-conjugated secondary antibodies instead of immunogold particles. The mapping patterns of net nitrogen were restricted to the outermost cell surface.

For Peer Review Only

Key words: antigen retrieval, immunolabeling, *Tannerella forsythensis*

For Peer Review Only

For electron microscopic immunocytochemistry, general ultrastructure sometimes has been sacrificed to obtain specific, efficient and dense labeling. Antigenicity often is lost by the conventional postfixation of tissue with OsO_4 (Roth et al. 1981). Omission of OsO_4, however, results in poor membrane contrast and thereby compromises visualization of fine structure. Therefore, several investigators have used potassium ferrocyanide-reduced OsO_4 to achieve excellent preservation of ultrastructure and good immunoreactivity of the antigens (Tamaki and Yamashina 1994, Tamatani et al. 1995). Postfixation by potassium ferrocyanide-reduced OsO_4 has been applied widely to obtain fine membrane structures with clear contrast for morphological observation by transmission electron microscopy (Doine et al. 1984, Rambourg et al. 1993).

Antigen retrieval can recover antigens masked by fixation, storage, processing and resin interactions. Such procedures have been used extensively for light and electron microscopy (Xiao et al. 1996, Shi et al. 2001, Calabria et al. 2010, Martins et al. 2011). Antigen retrieval involves heating in buffers at different pH and in the presence of enzymes (Cattoretti et al. 1993, von Wasielewski et al. 1994, Shi et al. 1995, Taylor et al. 1996, Pileri et al. 1997, Mighell et al. 1998). A common antigen retrieval treatment includes the use of citrate buffer, Tris-HCl containing 5% urea,

For Peer Review Only

and EDTA solutions combined with heating in a microwave oven or autoclave (Namimatsu et al. 2005). Citraconylation by citraconic anhydride was introduced as a method for reversible blocking of protein amino groups (Dixon and Perham 1968). Using this principle, Namimatsu et al. (2005) reported that by incorporating citraconic anhydride and heat, successful antigen retrieval in formalin fixed tissues is feasible. Because glutaraldehyde basically is similar to formaldehyde in its mechanism of action, these investigators explored whether the same method could work on glutaraldehyde fixed tissues for use in immunoelectron microscopy.

We observed earlier that 230 and 270 kDa proteins might be a component of the S-layer of bacteria based on the results of our immunoelectron microscopic study of 4% paraformaldehyde-0.05% glutaraldehyde fixation without OsO_4 or after freeze-substitution (Higuchi et al. 2000, Moriguchi et al. 2003). Sabet et al. (2003), however, reported that the S-layer consists of 200 and 210-kDa proteins. In their study, the bacterial cells were re-suspended in 0.1 M cacodylate buffer with 1% glutaraldehyde and postfixed with 1% OsO_4.

A large number of antigen particles and their clear localization are important requirements for optimal presentation of tissue antigen for immunohistochemistry. Therefore, we tried an antigen retrieval method that combined citraconic anhydride and microwave oven or autoclave

URL: http://mc.manuscriptcentral.com/tbih E-mail: biotech-histochem@louisville.edu

For Peer Review Only

heating for post-embedding immunoelectron microscopy; this resulted in better retention of specific gold-labeled particles binding and rich nitrogen, which reflects the presence of 3,3'-diaminobenzidine, tetrahydrochloride (DAB) moieties detected by energy-filtering transmission electron microscopy (EFTEM). That is, peroxidase-DAB reaction leads to DAB polymerization via nitrogen atoms (Vannier-Santos and Lins 2001). Two different modes of the EFTEM (Golecki and Heinrich 1991, Kortje et al. 1991, Fehrenbach et al. 1992, Huxham et al. 1992, Busch et al. 1993, Beckers et al. 1994) have been used for electron spectroscopic images (ESI) and electron energy-loss spectroscopy (EELS). Parallel-EELS is an additional tool. This procedure was performed using the commercially-available LEO LIBRA 120 Omega EFTEM.

For Peer Review Only

Materials and methods

Cell culture

T. forsythensis ATCC 43037 was obtained from A. Tanner (Forsyth Institute, Boston, MA). This strain was grown anaerobically for 7 days on Brucella agar (Difco Laboratories, Detroit, MI) supplemented with 5% laked-rabbit blood, 2.5 µg/ml hemin, 5.0 µg/ml menadione, 0.01% dithiothreitol, and 10 µg/ml *N*-acetylmuramic acid at 37˚ C. The bacteria were harvested by scraping colonies from Brucella agar plates. The cells were washed once with 10 mM Tris-HCl, pH 7.4, containing 0.15 M NaCl. The washed cells were disrupted by sonication at 5˚ C for 15 min with a Bioruptor UCD-200T (Cosmo Bio Co., Ltd., Tokyo, Japan) in the presence of proteinase inhibitors (0.25 mM *N*- α -*p*-tosyl-L-lysine chloromethyl ketone, 0.2 mM phenylmethylsulfonyl fluoride and 0.1 mM leupeptin).

Antigen preparation

Whole cell extracts were obtained as a supernatant after unbroken cells were removed by centrifugation at 1,000 x g for 10 min. Envelope and soluble fractions were separated by ultracentrifugation of the whole cell extracts at 143,000 x g for 60 min as described previously (Higuchi et al. 2000). The envelope fraction was subjected to sodium dodecylsulfate-polyacrylamide gel electrophoresis (SDS-PAGE) (Lugtenberg et al. 1975).

For Peer Review Only

The 270 kDa major protein was used as an antigen for preparing a specific antiserum. To do this, the 270 kDa band was cut from the SDS-PAGE preparative gel and purified. Antiserum against the 270 kDa protein was raised in a rabbit. The specificity of the antiserum was verified by Western blot analysis as described previously (Higuchi et al. 2000).

Cell preparation

T. forsythensis cells were fixed first with 4% paraformaldehyde-0.05% glutaraldehyde in phosphate-buffered saline, pH 7.4, (PBS) at 4˚ C for 60 min, then postfixed with 1% potassium ferricyanide-reduced OsO_4 at 4˚ C for 60 min. These samples were dehydrated and embedded in LR White (London Resin Co., Ltd., Berkshire, England). The resin was polymerized at 55˚ C for 24 h.

Antigen retrieval

Nickel grids (Veco, 200–mesh) with ultrathin sections of LR White embedded blocks were immersed in 1% citraconic anhydride solution (Nissin EM Co., Ltd., Tokyo, Japan), placed in a microwave oven (MI-77 Azumaya, Co., Tokyo, Japan) and heated on and off automatically to keep the temperature at 100˚ C for 15 min (net microwave irradiation of 11.7 min) or placed in an autoclave (MAC-280, ELK Corp., Tokyo, Japan) at 115˚ C for 30 min or 135˚ C for 15 min. After this, the grids in the

For Peer Review Only

citraconic anhydride solution were allowed to cool to room temperature for 30 min.

Immunogold labeling

After antigen retrieval, nonspecific staining was blocked by treatment for 30 min with 1% bovine serum albumin (BSA) in PBS. Immunogold reactions were carried out using an indirect method. The grids were treated for 12 h by inserting them in drops of antiserum diluted 500-fold in 1% BSA-PBS. After two washes with PBS, the grids were incubated for 1 h in goat anti-rabbit IgG labeled with 20 nm gold, secondary antibodies (EY Laboratories, Inc., San Mateo, CA) diluted 50 fold in 1% BSA-PBS, and washed twice with PBS. The immunolabeled sections were counterstained with uranyl acetate and lead citrate. They then were examined under an electron microscope JEM 1210 (JEOL, Tokyo, Japan).

ESI and parallel-EELS

After antigen retrieval, the grids treated in drops of antiserum were incubated for 12 h in HRP-conjugated secondary antibodies instead of immunogold particles. The immuno-HRP labeled sections then were incubated for 1 h in DAB reaction solution consisting of 0.1% DAB and 0.001% H_2O_2. To gain ESI and parallel-EELS of the nitrogen, which is reflected by the presence of DAB moieties, we used the EFTEM, Carl

For Peer Review Only

Zeiss LIBRA 120 (Carl Zeiss, Oberkochen, Germany) operated at 120 kV. To analyze ESI, a slow scan CCD camera linked to a computer recorded energy-filtered images of identical elements. The transmission image, a zero-loss image using only a non-scattered electron beam, was recorded. The ESI of the nitrogen was obtained from the ΔE_{max} at the 410 eV edge of K edge. To identify quantitatively the edge, we removed the background using a three-window method. The corresponding pixel signals were recorded for the first window, ΔE_{w1}, at 382 eV and the second window, ΔE_{w2}, at 350 eV below the edge.

Additional tool parallel-EELS is a technique for the rapid analysis of radiation sensitive specimens.

For Peer Review Only

Results

Immunogold labeling

In control sections without antigen retrieval, the cell wall consisted of a cytoplasmic membrane and an outer membrane with two electron-dense layers, as well as an S-layer in which the cells were enclosed. The S-layer showed serrated structural subunits. Moreover, immunogold particles were localized at the outermost cell surface where the S-layer was present (Fig. 1).

Immunogold particles that had been autoclaved (115˚ C or 132˚ C) or microwaved (100˚ C with citraconic anhydride) were observed by electron microscopy. Our ultrastructural observation of both retrieval methods revealed moderately decreased cytoplasm (Figs. 2a,b,d and 3a,c) compared to the control (Fig. 1). There was no damage to the ultrastructural integrity of the cytoplasmic membrane or outer membrane. Each membrane consisted of two electron-dense layers (Figs. 2c,e and 3b,d). In all heating retrievals with citraconic anhydride, the reactivity of immunogold particles was better than that of the controls, which permitted clear observation of antigen retrieval effects. (Figs. 2 and 3).

For Peer Review Only

ESI and parallel-EELS

The ESI and parallel-EELS analysis showed the distribution of the nitrogen in the cytoplasm of *T. forsythensis* without microwave antigen retrieval at 100˚ C. The EFTEM produced a zero-loss transmission image (Fig. 4a). The distribution of net nitrogen was demonstrated (Fig. 4b) using the three-window method at ΔE_{w1} (Fig. 4e), ΔE_{w2} (Fig. 4d) and ΔE_{max} 410ev of K edge of nitrogen (Fig. 4f). Figure 4c shows parallel-EELS analysis of the circle in Fig. 4b. A small amount of endogenous nitrogen was found in the cytoplasm. On the other hand, the same ESI and parallel-EELS analysis showed the distribution of nitrogen in the cytoplasm of *T. forsythensis* after microwave antigen retrieval at 100˚ C using 1% citraconic anhydride with or without the DAB reaction solution (consisting of 0.1% DAB and 0.001% H_2O_2). The microwave antigen retrieval treatment caused the nitrogen signals to disappear completely (data not shown) compared to Fig 4, which shows endogenous nitrogen distribution.

Finally, ESI analysis demonstrated the distribution of nitrogen (the DAB reaction solution consisting of 0.1% DAB, 0.001% H_2O_2 and HRP-conjugated secondary antibodies instead immunogold particles) onto a structural image in the cytoplasm of *T. forsythensis* (after microwave antigen-retrieval treatment at 100˚ C consisting of 1% citraconic anhydride). The EFTEM produced a zero-loss transmission image (Fig. 5a). The

For Peer Review Only

distribution of net nitrogen was demonstrated (Fig. 5b) by using the three-window method at ΔE_{w1} (Fig. 5e), ΔE_{w2} (Fig. 5d) and ΔE_{max} 410ev of K edge (Fig. 5f). Nitrogen distribution (Fig 5b) is in red, and superimposed to the zero-loss transmission image (Fig. 5a), strictly corresponded with the outermost cell surface where the S-layer was present (Fig. 5g). Figure 5c shows parallel-EELS analysis of the circled area of Fig. 5b.

For Peer Review Only

Discussion

The human oral cavity harbors more than 500 species of bacteria. Periodontitis, a bacterial inflammatory disease that leads to tooth loss, is believed to result from infection by a select group of Gram-negative periodontal pathogens including *Porphyromonas gingivalis, Treponema denticola,* and *Tannerella forsythensis*. *T. forsythensis* is characterized by two unique protein bands with molecular weights of more than 205 kDa as shown by SDS-PAGE (Tanner et al. 1986). The upper protein band is the 270 kDa protein. Ultrastructurally, many bacteria and archaea have a typical S-layer consisting of serrated subunits outside the outer membrane (Tanner et al. 1986, Kerosuo 1988, Sleytr and Beveridge 1999, Sara and Sleytr 2000). We confirmed by electron microscopy that the S-layer was located outside the outer membrane. The objective of our earlier study was to investigate any relationship between the S-layer and the 270 kDa protein in *T. forsythensis* (Higuchi et al. 2000). The cells were fixed with 4% paraformaldehyde-0.05% glutaraldehyde containing 4% sucrose and 0.05% calcium chloride, and postfixed with 0.5% uranyl acetate. We found that immunogold particles were localized at the outermost cell surface when antiserum was used, but not when pre-immune serum was used (Higuchi et al. 2000). In the work reported here, we applied antigen retrieval using citraconic anhydride solution and microwave or autoclave heating for post-

For Peer Review Only

embedding immunoelectron microscopy. Citraconic anhydride reacts with the free amino groups of proteins and replaces the NH^{+3} groups of lysyl residues with negatively-charged carboxyl groups (Dixon and Perham 1968, Habeeb and Atassi 1970).

Namimatsu et al. (2005) explored the use of citraconic anhydride as a reversible blocker of protein amino groups during formaldehyde and glutaraldehyde tissue fixation. Citraconic anhydride b can chemically modify amino groups that are the main targets of these fixatives and the reaction can be reversed later for immunoreactions. Like formaldehyde, glutaraldehyde reacts mainly with lysyl residues; some reaction occurs also with tyrosyl, histidyl, and sulfhydryl residues. It is possible that this approach could make possible the preservation of both ultrastructure and immunoreactivity for formalin fixed tissues. Similarly, antigen retrieval permits successful pre-embedding immunoelectron microscopy of glutaraldehyde fixed tissues (Dai et al. 2004). Moreover, Anthony et al. (2010), exploring a suggestion by Namimatsu et al. (2005) that citraconic anhydride might be a suitable antigen retrieval reagent, compared the immunostaining of 65 common diagnostic antigens following microwave antigen retrieval and confirmed that citraconic anhydride is a useful antigen retrieval compound, especially when used with microwave irradiation.

For Peer Review Only

In addition to finding that immunogold particles were clearly localized at the outermost cell surface where the S-layer is located, we observed by electron microscopy that there was moderately decreased cytoplasm compared to controls after both heating retrieval methods with citraconic anhydride. There was no damage to the ultrastructural integrity of the cytoplasmic membrane or outer membrane; each membrane consisted of two electron-dense layers. We concluded that antigen retrieval at high temperature in citraconic anhydride may damage the cytoplasmic ultrastructure.

The use of peroxidase and DAB for ultrastructural cytochemistry was introduced by Graham and Karnovsky (1966a,b) to trace endocytosis, but it also has been employed for demonstrating catalase (Moriguchi et al. 1984) and cytochrome oxidase (Hirai et al. 1989, Moriguchi et al. 1998), and for detecting endogenous peroxidase activity (Moriguchi et al. 2000). Oxidation causes DAB polymerization via nitrogen atoms and the resulting polymer is highly osmiophilic and insoluble, which allows easy identification of electron-dense precipitates of the enzymatic reaction product with minimal diffusion artifacts (Vannier-Santos and Lins 2001). Therefore, we used EFTEM to visualize also the enzyme reaction product (Moriguchi et al. 2008). The immunocytochemical localization of colloidal gold particle-conjugated secondary antibodies corresponded to the nitrogen

For Peer Review Only

identified by the maximal electron energy loss at 410 eV (K edge) in the ESI analysis. As reported earlier, ESI and EELS analyses under the EFTEM have been applied to demonstrate isolated ferritin particles (Beckers et al. 1994), calcium elements of plant root caps (Busch et al. 1993), iodine-containing anti-cancer drug meta-iodobenzyl guanidine (Huxham et al. 1992), phosphorus in mammalian lung parenchyma (Fehrenbach et al. 1992) and cyanobacteria (Golecki and Heinrich 1991), and calcium-ATPase in synaptic terminals (Kortje et al. 1991). These methods are fairly reliable and useful for analyzing several elements in biological materials; they are especially useful for mapping analysis compared to X-ray microanalysis. In addition, the three-window method easily removes the background. Moreover, the parallel-EELS is metods for quickly analyzing radiosensitive sample (Kortje 1994, Moriguchi et al. 2011) and this enabled us to confirm that the electron-dense materials along the S-layer contained nitrogen.

The S-layer in *T. forsythensis* has been suggested to be associated with hemagglutination, adhesion and invasion of host cells; however, its precise functions remain unknown. Sakakibara et al. (2007) suggested that lack of the S-layer had a minor effect on hemagglutination. Moreover, hemagglutination inhibition by S-layer-specific antisera raised against the 230 and/or 270 kDa proteins was almost the same as that produced by the

For Peer Review Only

control pre-immune serum. Thus the S-layer seemed to have a marginal association with the hemagglutination. Because thin section microscopy revealed that the cell surfaces of the single mutants (Δ 230 and Δ 270) were partially covered with substances like the S-layer, an abnormal state of the cell surface could hinder hemagglutination. In the double mutant (Δ 230-270), which lacks the S-layer, the putative hemagglutinin might be fully exposed and functioning. By contrast, the S-layer proteins in *T. forsythensis* clearly were responsible for adhesion to the host cells. The S-layer protein-deficient mutants lost adherence almost completely.

For Peer Review Only

References

Beckers AL, de Bruijn WC, Jongkind JF, Cleton-Soeteman MI, Apkarian RP, Gelsema ES (1994) Energy-filtering transmission electron microscopy as a tool for structural and compositional analysis of isolated ferritin particles. *Scanning Microsc. Suppla.* 8: 261-274.

Busch MB, Kortje KH, Rahmann H, Sievers A (1993) Characteristic and differential calcium signals from cell structures of the root cap detected by energy-filtering electron microscopy (EELS/ESI). *Eur. J. Cell Biol.* 60: 88-100.

Calabria LK, Teixeira RR, Coelho Goncalves SM, Passos Lima AB, Santos AA, Dai W, Sato S, Ishizaki M, Wakamatsu K, Namimatsu S, Sugisaki Y, Ghazizadeh M (2004) A new antigen retrieval method using citraconic anhydride for immunoelectron microscopy: localization of surfactant pro-protein C (proSP-C) in the type II alveolar epithelial cells. *J. Submicrosc. Cytol. Pathol*. 35: 219-224.

Cattoretti G, Pileri S, Parravicini C, Becker MHG, Poggi S, Bifulco C, Key G, D'Amato L, Sabattini E, Feudale E, Reynolds F, Gerdes J, Rilke F (1993) Antigen unmasking on formalin-fixed, paraffin-embedded tissue sections. *J. Pathol*. 171: 83-98.

For Peer Review Only

Dixon HB, Perham RN (1968) Reversible blocking of amino groups with citraconic anhydride. *Biochem. J.* 109: 312-314.

Doine AI, Oliver C, Hand AR (1984). The Golgi apparatus and GERL during postnatal differentiation of rat parotid acinar cells: an electron microscopic cytochemical study. *J. Histochem. Cytochem.* 32: 477-485.

Fehrenbach H, Richter J, Schnabel PA (1992) Electron spectroscopic study (ESI, EELS) of Nanoplast-embedded mammalian lung. *J. Microsc.* 166: 401-416.

Golecki JR, Heinrich UR (1991) Ultrastructural and electron spectroscopic analyses of cyanobacteria and bacteria. *J. Microsc.* 162: 147-154.

Graham RC Jr, Karnovsky MJ (1966a) Glomerular permeability. Ultrastructural cytochemical studies using peroxidases as protein tracers. *J. Exp. Med.* 124: 1123-1134.

Graham RC Jr, Karnovsky MJ (1966b) The early stages of absorption of injected horseradish peroxidase in the proximal tubules of mouse kidney: ultrastructural cytochemistry by a new technique. *J. Histochem. Cytochem.* 14: 291-302.

For Peer Review Only

Habeeb AF, Atassi MZ (1970) Enzymic and immunochemical properties of lysozyme. Evaluation of several amino group reversible blocking reagents. *Biochemistry* 9: 4939-4944.

Higuchi N, Murakami Y, Moriguchi K, Ohno N, Nakamura H, Yoshimura F (2000) Localization of major, high molecular weight proteins in *Bacteroides forsythus*. *Microbiol. Immunol*. 44: 777-780.

Hirai KI, Ogawa K, Wang GY, Ueda T (1989) Varied cytochrome oxidase activities of the alveolar type I, type II and type III cells in rat lungs: quantitative cytochemistry. *J. Elect. Microsc.* (*Tokyo*) 38: 449-456.

Huxham IM, Gaze MN, Workman P, Mairs RJ (1992) The use of parallel EEL spectral imaging and elemental mapping in the rapid assessment of anti-cancer drug localization. *J. Microsc*. 166: 367-380.

Kerosuo E (1988) Ultrastructure of the cell envelope of *Bacteroides forsythus* strain ATCC 43037T. *Oral Microbiol. Immunol*. 3: 134-137.

Kortje KH (1994) Image-EELS: a synthesis of energy-loss analysis and imaging. *Scanning Microsc*. 8: 277-287.

Kortje KH, Kortje D, Rahmann H (1991) The application of energy-filtering electron microscopy for the cytochemical localization of Ca^{++}-ATPase activity in synaptic terminals. *J. Microsc. Suppl*. 162: 105-114.

For Peer Review Only

Leong AS, Haffajee Z (2010) Citraconic anhydride: a new antigen retrieval solution. *Pathology* 42: 77-81.

Lugtenberg B, Meijers J, Peters R, van der Hoek P, van Alphen L (1975) Electrophoretic resolution of the "major outer membrane protein" of *Escherichia coli* K12 into four bands. *FEBS Lett.* 58: 254-258.

Martins AR, Espindola FS (2010) Comparative analysis of two immunohistochemical methods for antigen retrieval in the optical lobe of the honeybee *Apis mellifera*: myosin-V assay. *Biol. Res.* 43:7-12.

Martins AR, Zanella CA, Zucchi FC, Dombroski TC, Costa ET, Guethe LM, Oliveira AO, Donatti AL, Neder L, Chimelli L, De Nucci G, Lee-Ho P, Murad, F (2011) Immunolocalization of nitric oxide synthase isoforms in human archival and rat tissues, and cultured cells. *J. Neurosci. Methods.* In press.

Mighell AJ, Hume WJ, Robinson PA (1998) An overview of the complexities and subtleties of immunohistochemistry. *Oral. Dis*. 4: 217-223.

Moriguchi K, Higashi N, Kitagawa S, Takase K, Ohya N, Uyeda T, Hirai KI (1984) Differentiation of human pulmonary alveolar epithelial

For Peer Review Only

cells revealed by peroxisome changes in pulmonary proteinosis. *Exp. Mol. Pathol*. 40: 262-270.

Moriguchi K, Utsumi M, Ohno N (1998) Mitochondrial fixation for the detection of cytochrome oxidase activity using microwave irradiation. *Okajimas Folia Anat. Jpn*. 74: 207-215.

Moriguchi K, Utsumi M, Hanamura H, Ohno N (2000) Peroxidase activity in the submandibular gland of the house musk shrew, *Suncus murinus* (Soricidae, Insectivora). *Okajimas Folia Anat. Jpn*. 77: 29-33.

Moriguchi K, Higuchi N, Murakami Y, Yoshimura F, Nakamura H, Ohno N (2003) A morphological and immunolabeling study of freeze-substituted *Bacteroides forsythus*. *Biotech. & Histochem*. 78: 129-133.

Moriguchi K, Jogahara T, Kurihara T, Iwami J, Higuchi N, Murakami Y, Maeda H, Yoshimura F, Nakamura H, Ohno N (2008) Immunocytochemical approach for surface layer proteins of freeze-substituted *Tabberella forsythensis* by energy-filtering transmission electron microscopy. *Okajimas Folia Anat. Jpn*. 85: 67-72.

Moriguchi K, Muraji N, Shigemori T, Mitamura Y, Maeda H, Tanaka Y, Kawai T, Ohno N (2011) Analysis of the relationship between mean

For Peer Review Only

free path and Ca intensity in enamel sections using EFTEM. *J. Elect. Microsc. Tech. Med. Biol*. 25: 1-4

Namimatsu S, Ghazizadeh M, Sugisaki Y (2005) Reversing the effects of formalin fixation with citraconic anhydride and heat: a universal antigen retrieval method. *J. Histochem. Cytochem*. 53: 3-11.

Pileri SA, Roncador G, Ceccarelli C, Piccioli M, Briskomatis A, Sabattini E, Ascani S, Santini D, Piccaluga PP, Leone O, Damiani S, Ercolessi C, Sandri F, Pieri F, Leoncini L, Falini B (1997) Antigen retrieval techniques in immunohistochemistry: comparison of different methods. *J. Pathol*. 183: 116-123.

Rambourg A, Clermont Y, Chretien M, Olivier L (1993) Modulation of the Golgi apparatus in stimulated and nonstimulated prolactin cells of female rats. *Anat. Rec*. 235: 353-362.

Roth J, Bendayan M, Carlemalm E, Villiger W, Garavito M (1981) Enhancement of structural preservation and immunocytochemical staining in low temperature embedded pancreatic tissue. *J. Histochem. Cytochem*. 29: 663-671.

Sakakibara J, Nagano K, Murakami Y, Higuchi N, Nakamura H, Shimozato K, Yoshimura F (2007) Loss of adherence ability to human

For Peer Review Only

gingival epithelial cells in S-layer protein-deficient mutants of *Tannerella forsythensis*. *Microbiology* 153: 866-876

Sabet M, Lee SW, Nauman RK, Sims T, Um HS (2003) The surface (S-) layer is a virulence factor of *Bacteroides forsythus*. *Microbiology* 149: 3617-3627.

Sara M, Sleytr UB (2000) S-Layer proteins. *J. Bacteriol*. 182: 859-868.

Shi SR, Cote RJ, Taylor CR (2001) Antigen retrieval techniques: current perspectives. *J. Histochem. Cytochem*. 49: 931-937.

Shi SR, Imam SA, Young L, Cote RJ, aylor CR (1995) Antigen retrieval immunohistochemistry under the influence of pH using monoclonal antibodies. *J. Histochem. Cytochem*. 43: 193-201.

Sleytr UB, Beveridge TJ (1999) Bacterial S-layers. *Trends Microbiol*. 7: 253-260.

Tamaki H, Yamashina S (1994) Improved method for post-embedding cytochemistry using reduced osmium and LR white resin. *J. Histochem. Cytochem*. 42: 1285-1293.

For Peer Review Only

Tamatani R, Taniguchi Y, Kawarai Y (1995) Ultrastructural study of proliferating cells with an improved immunocytochemical detection of DNA-incorporated bromodeoxyuridine. *J. Histochem. Cytochem*. 43: 21-29.

Tanner ACR, Listgarten MA, Ebersole JL, Strzempko MN (1986) *Bacteroides forsythus* sp. nov., a slow-growing, fusiform *Bacteriodes* sp. from the human oral cavity. *Int. J. Syst. Bacteriol*. 36: 213-218.

Taylor CR, Shi SR, Chen C, Young L, Yang C, Cote RJ (1996) Comparative study of antigen retrieval heating methods: microwave, microwave and pressure cooker, autoclave, and steamer. *Biotech. & Histochem*. 71: 263-270.

Vannier-Santos MA, Lins U (2001) Cytochemical techniques and energy-filtering transmission electron microscopy applied to the study of parasitic protozoa. *Biol. Proced. Online* 3: 8-18.

von Wasielewski R, Werner M, Nolte M, Wilkens L, Georgii A (1994) Effects of antigen retrieval by microwave heating in formalin-fixed tissue sections on a broad panel of antibodies. *Histochemistry* 102: 165-172.

Xiao JC, Adam A, Ruck P, Kaiserling E (1996) A comparison of methods for heat-mediated antigen retrieval for immunoelectron

For Peer Review Only

microscopy: demonstration of cytokeratin No. 18 in normal and neoplastic hepatocytes. *Biotech. & Histochem*. 71: 278-285.

For Peer Review Only

Fig. 1. Immunogold-labeled *T. forsythensis* cells. Control section without antigen retrieval treatment. Cytoplasmic membrane (CM) and outer membrane (OM) consisted of two electron-dense layers. Serrated subunits of S-layer (S) are shown.

Fig. 2. Low (b, d) and high (a, c, e) magnification micrographs of immunogold-labeled *T. forsythensis* cells after antigen retrieval by heating with the autoclave. a) Autoclaved at 115˚ C with 1% citraconic anhydride. b and c) Autoclaved at 132˚ C with distilled water. d and e) Autoclaved at 132˚ C with 1% citraconic anhydride. Moderately decreased cytoplasm (a, b) compared to control cytoplasm (Fig. 1) without damage to the ultrastructural integrity of the cytoplasmic membrane and outer membrane (c, e). Immunogold-particles in a, c, e showed greater reactivity than the control (Fig. 1). CM, cytoplasmic membrane; OM, outer membrane; S, S-layer.

Fig. 3. Low (a, c) and high (b, d) magnification micrographs of immunogold-labeled *T. forsythensis* cells after antigen retrieval by heating with the microwave oven. Microwaved at 100˚ C with 1% citraconic anhydride. Moderately decreased cytoplasm (a, c) compared to control cytoplasm (Fig. 1) without damage to the ultrastructural integrity of cytoplasmic membrane and outer membrane (b, d). Immunogold-particles

For Peer Review Only

in (b) and (d) showed greater reactivity than the control (Fig. 1). CM, cytoplasmic membrane; OM, outer membrane; S, S-layer.

Fig. 4. ESI and parallel-EELS analysis showed the distribution of nitrogen in the cytoplasm of *T. forsythensis* without microwave treatment at 100˚ C; cells only. A small amount of endogenous nitrogen was observed in the cytoplasm. a) Zero-loss transmission image. b) Background removed net ΔE_{max} 410 eV. c) Parallel-EELS analysis of the circled area of Fig. 4b. d) The second window of ΔE_{w2} 350 eV. e) The first window of ΔE_{w1} 382 eV of nitrogen. f) ΔE_{max} 410 eV of K edge of nitrogen.

Fig. 5. ESI using three-window method and parallel-EELS for *T. forsythensis* cells incubated in DAB medium with H_2O_2 and DAB. Nitrogen distribution corresponded to the outermost cell surface, the S-layer. a) Zero-loss transmission image. b) Background removed net ΔE_{max} 410 eV. c) Parallel-EELS analysis of the circled area in Fig. 5b. d) The second window of ΔE_{w2} 350 eV t. e) The first window of ΔE_{w1} 382 eV of nitrogen. f) ΔE_{max} 410 eV of K edge of nitrogen. g) Superimposed image of nitrogen distribution over the zero-loss image. CM, cytoplasmic membrane; OM, outer membrane; S, S-layer.

For Peer Review Only

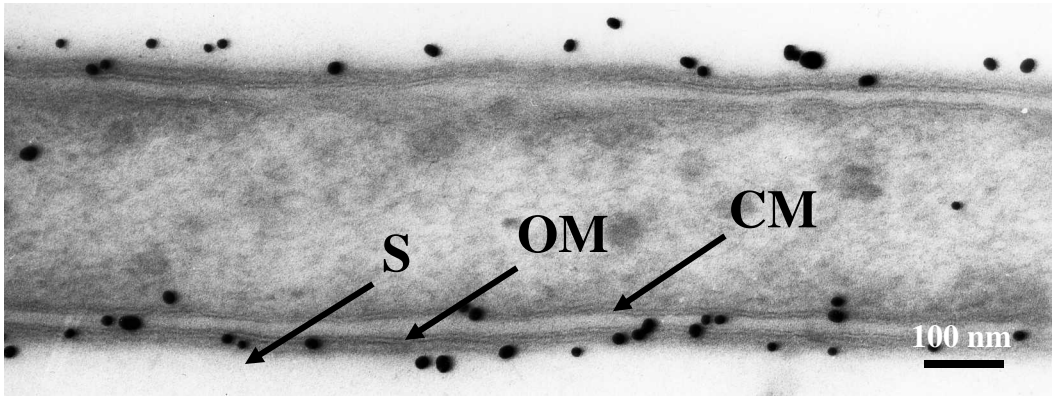

Fig. 1

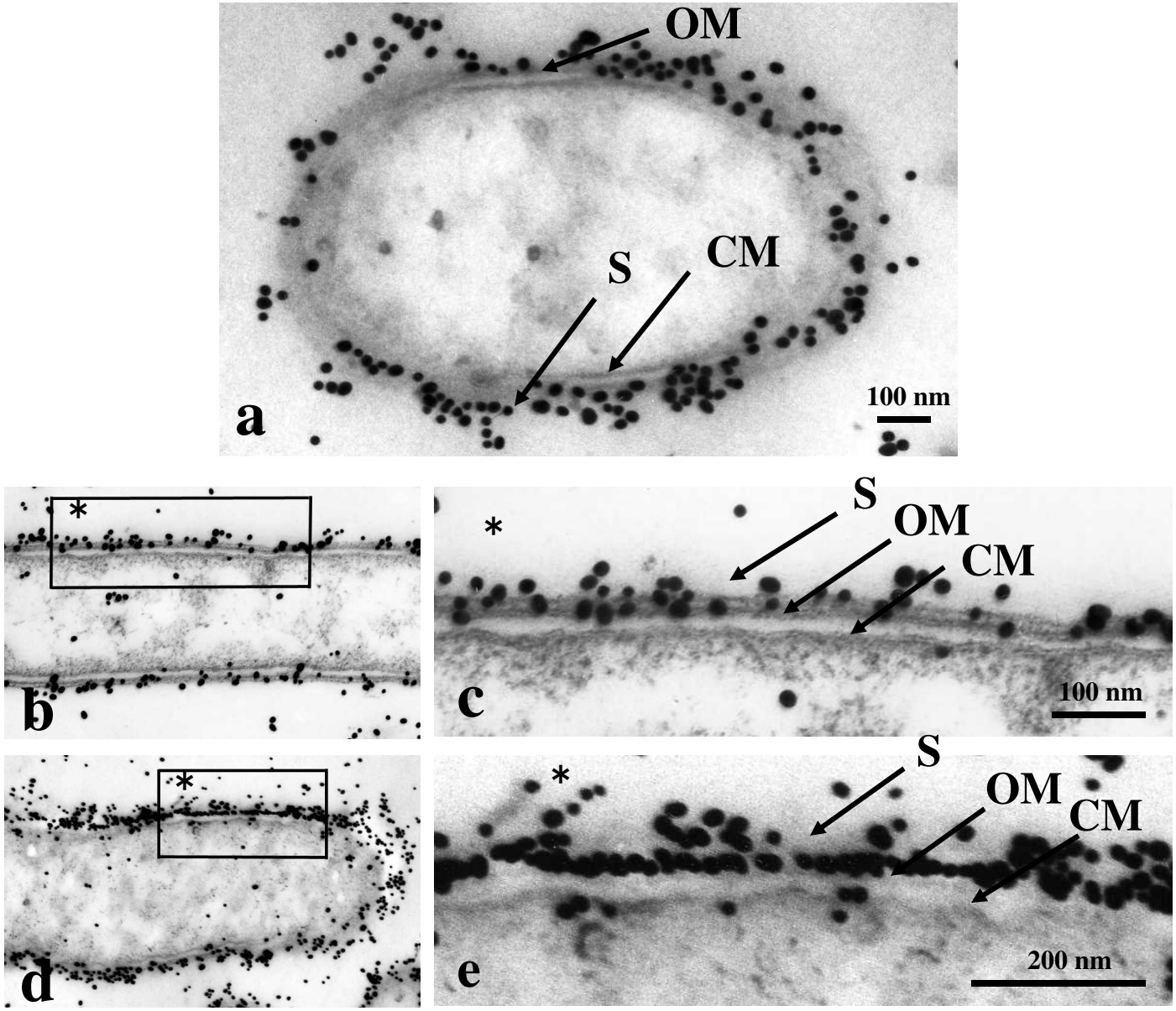

Fig. 2

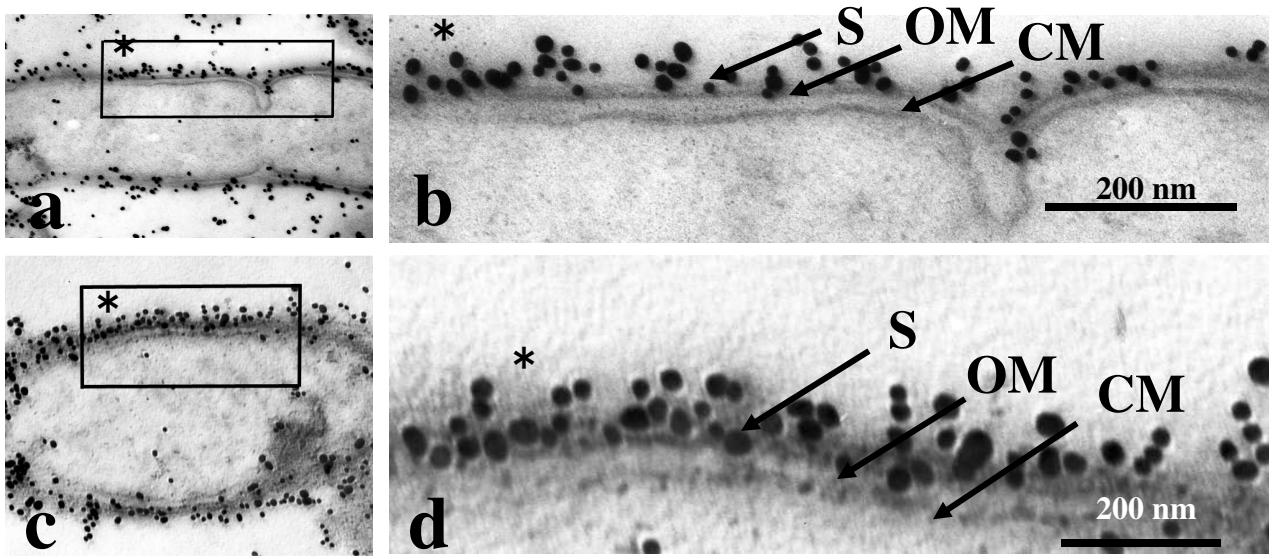

Fig. 3

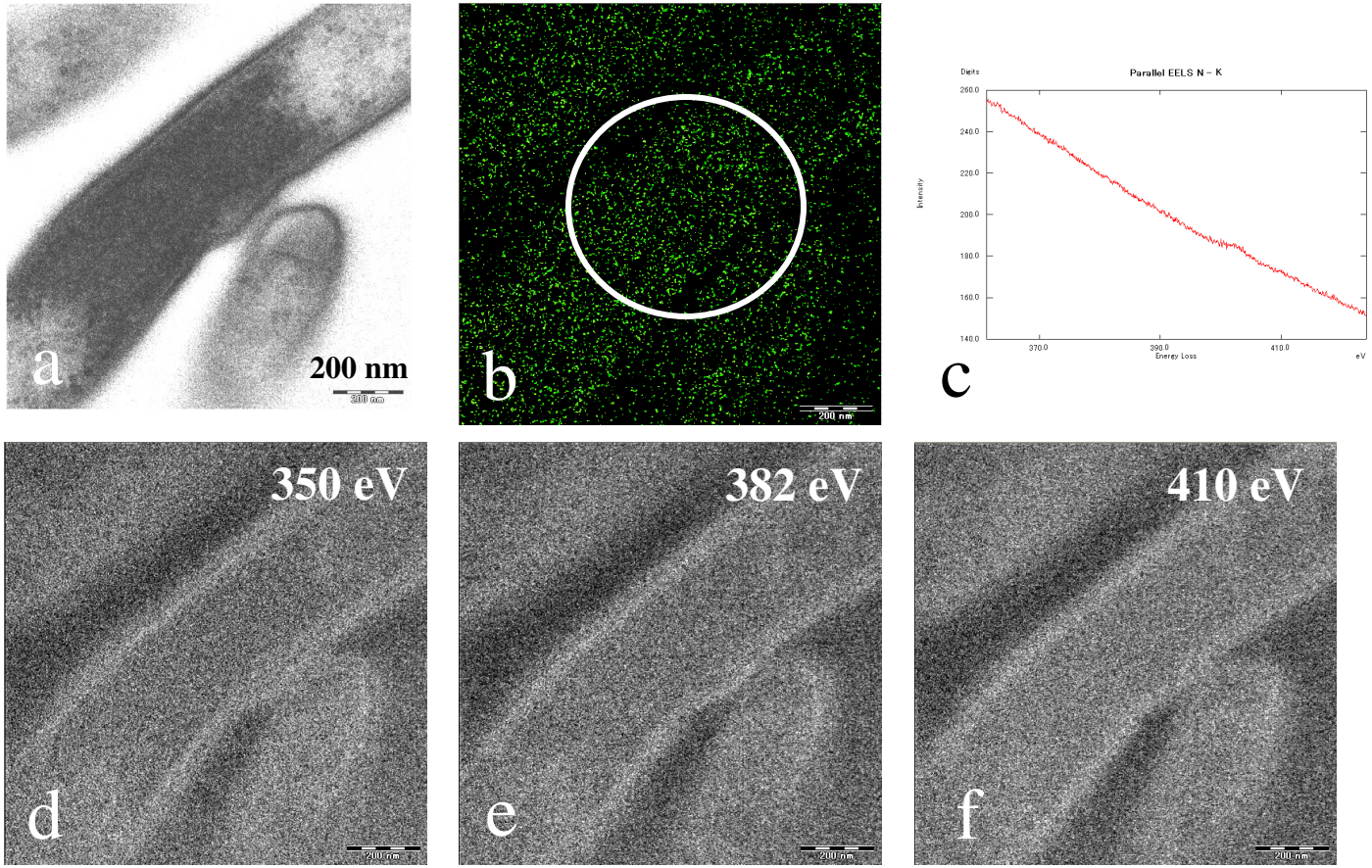
a
200 nm
b
c
Parallel EELS N – K
Counts
Intensity
260.0
240.0
220.0
200.0
180.0
160.0
140.0
370.0
390.0
410.0
Energy Loss
eV
350 eV
d
382 eV
e
410 eV
f

Fig. 4

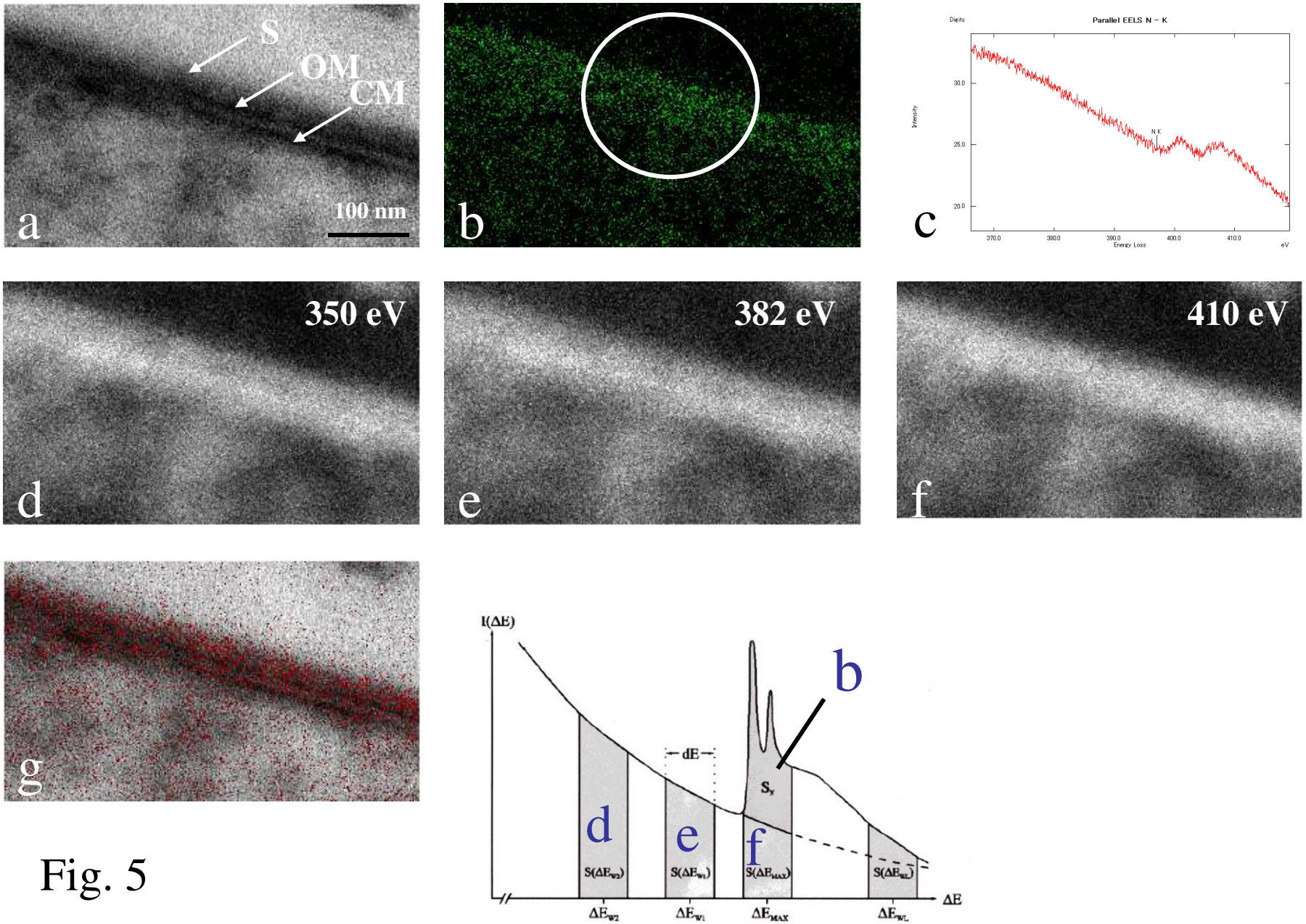
S
OM
CM
100 nm
a
b
c
Parallel EELS N – K
Digits
Intensity
N K
Energy Loss
eV
350 eV
d
382 eV
e
410 eV
f
g
I(ΔE)
b
dE
d
e
f
S(ΔE_W2)
S(ΔE_W1)
S(ΔE_MAX)
S(ΔE_WL)
ΔE_W2
ΔE_W1
ΔE_MAX
ΔE_WL
ΔE

Fig. 5